International Journal of Sustainability in Research (IJSR)
Vol. 3, No. 5, 2025: 361-370

Microstructural and Elemental Characterization of Aluminium Alloy A356/Cow Horn Particle Composite Using SEM and EDX Techniques

Sunday Chimezie Anyaora[1], Stephen A. Takim[2], Madubueze Sunday Ofochebe[3]*, Paul Tochukwu Agu[4]
[1, 3, 4]Department of Mechanical Engineering, Faculty of Engineering in Nnamdi Azikiwe University, Awka, Anambra State, Nigeria
[2]Department of Mechanical Engineering, University of Cross River State, Unicross Calabar, Cross River State, Nigeria
Corresponding Author: Madubueze Sunday Ofochebe
sm.ofochebe@unizik.edu.ng

A R T I C L E I N F O

Keywords: Aluminium Alloy A356, Cow Horn Particulates, Microstructure, SEM, EDX

Received: 21, July
Revised: 20, August
Accepted: 30, September

A B S T R A C T

Research into substitute reinforcements for metal matrix composites has increased due to the engineering and automotive sectors' increasing need for lightweight, strong, and reasonably priced materials. Despite their effectiveness, conventional reinforcements like silicon carbide and alumina are costly and harmful to the environment. To examine the machining behavior of aluminum alloy A356 reinforced with cow horn particles (0–20%), the study used an experimental methodology. To guarantee structural integrity, spark plasma sintering was used to create the composites at 550°C and 30 MPa under vacuum. Using HSS and HCS tools, machining experiments were carried out on a Universal Turning Machining Center. Response Surface Methodology was used to improve parameters such as cutting speed, feed rate, and depth of cut. Using a Phenom ProX model, scanning electron microscopy (SEM) was used to analyze surface morphology, and energy dispersive X-ray spectroscopy (EDX) was used to characterize the ideal composite sample's elements and composition. Scanning Electron Microscope (SEM) results revealed reduced wear in CHp composites, as larger particles improved interfacial bonding, toughness, and resistance to plastic deformation compared to the unreinforced alloy. The study demonstrates that CHp reinforcement offers an eco-friendly and economical approach to enhancing the performance of aluminum alloys for industrial applications.

DOI: https://doi.org/10.59890/ijsr.v3i5.165
ISSN-E: 3025-7379
https://dmimultitechpublisher.my.id/index.php/ijsr

INTRODUCTION

The automotive and aerospace sectors make extensive use of the aluminum alloy A356 due to its exceptional castability, strength, and low weight. Nonetheless, the ongoing need for robust and ecological materials has prompted the usage of agro-waste particles as reinforcements. Cow horn particle (CHp) has gained interest as a cost-effective and sustainable reinforcement. When added to A356, it can improve specific strength, hardness, and wear resistance while also reducing waste. Notwithstanding these possible advantages, there are still difficulties in limiting porosity and agglomeration, obtaining uniform particle dispersion, and establishing sufficient interfacial bonding. Improving the mechanical and tribological properties of A356 requires an understanding of how CHp influences its microstructure and elemental composition (Ochieze et al., 2018; Oguntuase et al., 2022).

Studies on A356 reinforced with cow horn particles reveal that the amount of reinforcement and processing technique have a significant impact on microstructure alterations. Grain structure and inclusion distribution are changed when CHp is added to A356, according to studies. While inclusion clusters, a duller grain appearance, and localized porosity are the results of greater fractions, grains stay fine and compact at lower CHp percentages. When CHp is utilized excessively, these changes are linked to decreased wettability and particle agglomeration. As a result, mechanical attributes, including wear resistance and hardness, increase at moderate CHp levels but start to decrease at excessively high reinforcement content (Ochieze et al., 2018).

The impact of CHp on the composite is further elucidated by elemental characterisation. While trace metals, including magnesium, manganese, iron, titanium, and copper, are present in both the base alloy and the composites, energy dispersive spectroscopy and spectrographic tests show that silicon and aluminum continue to be the dominant constituents in the A356 matrix. These factors affect how strengthening precipitates occur and how the composite reacts to age-hardening. According to Oguntuase et al. (2022), microstructural analysis revealed that the addition of CHp created areas of chemical heterogeneity that impacted localized hardness and strength, even if the aluminum content remained predominant.

The overall characteristics of the composite are greatly influenced by the processing methods used. Common methods for creating A356–CHp composites include powder metallurgy, stir casting, and spark plasma sintering. Controlled powder pathways and spark plasma sintering have demonstrated reduced porosity and improved particle bonding in comparison to conventional stir casting. Their interfacial reaction zones are finer, and their particle distribution is more uniform. The wettability of CHp with molten aluminum is, however, generally limited by its organic and mineral makeup. To solve this, wetting chemicals like magnesium or surface treatments have been used to improve the bonding between the cow horn particles and the aluminum matrix (Nwobi-Okoye & Ochieze, 2018).

When compared to unreinforced A356, tribological and mechanical studies show that moderate levels of CHp, usually between 3 and 10 weight percent, improve hardness, tensile strength, compressive strength, and wear

rate. These enhancements result from the decrease in metal-to-metal contact during sliding and the load transfer mechanism, in which the cow horn particles share the applied stress with the aluminum matrix. Very high reinforcement levels, however, have the potential to decrease ductility, encourage particle agglomeration, and increase brittleness. By fine-tuning the precipitate distribution within the matrix, heat treatment—especially artificial ageing—improves hardness and wear resistance, according to optimization studies (Nwobi-Okoye et al., 2019).

LITERATURE REVIEW

Microstructural examination through optical and scanning electron microscopy confirms that CHp promotes nucleation during solidification, which results in grain refinement. This refinement improves mechanical strength due to a higher grain boundary area that resists dislocation motion. Nonetheless, the extent of refinement depends on proper stirring, particle size, and uniform temperature distribution during fabrication. Surface analyses further demonstrate that good interfacial bonding between CHp and A356 is necessary for effective stress transfer. Poor bonding leads to weak interfaces, which act as crack initiation sites during loading (Le et al, 2024). There is a growing need to develop cost-effective and eco-friendly composites that enhance the mechanical and wear properties of aluminium alloys used in automotive and aerospace industries. Although several studies examined aluminium-based composites with agro-waste reinforcements, limited work has explored cow horn particles using advanced microstructural and elemental techniques such as SEM and EDX. Previous research often reported uneven particle dispersion, weak interfacial bonding, and incomplete characterization of elemental distribution (Ochieze et al., 2018; Oguntuase et al., 2022). This study is therefore necessary to provide a detailed understanding of how cow horn particles influence the microstructure and composition of A356 composites.

METHODOLOGY

The study employed an experimental approach to investigate the machining behavior of Aluminum Alloy A356 reinforced with cow horn particulates (xCHp) at varying proportions (0–20%). The composite samples were fabricated using the spark plasma sintering technique at 550°C and 30 MPa, maintaining a vacuum of 2–10 torr to ensure material integrity. Each sample was cylindrical, measuring 100 mm in diameter and 5 mm in thickness, and processed under a controlled heating and cooling rate of 100°C per minute to achieve uniformity.

The materials used included Aluminum alloy A356, High-Speed Steel (HSS), and high-carbon steel (HCS) cutting tools, each with specific chemical compositions outlined in the study. Experiments were performed using a Universal Turning Machining Centre (Mikrotools DT 110), while measurements were taken using a surface tester, vernier caliper, and weighing balance.

Supporting equipment, such as the crucible, stirrer, conical hopper, and mould, facilitated the stir casting process and ensured uniform dispersion of particulates. The crucible was used to hold molten metal, while the stirrer operating at 300 rpm promoted vortex formation for homogeneous reinforcement distribution. The preheated mould (500°C for one hour) minimized porosity, and the lathe machine was employed for final finishing and dimensional accuracy.

The experimental design followed an Optimal Custom Design under the Response Surface Methodology (RSM) using Design Expert Software 11.0. This design allowed optimization of three machining parameters—cutting speed (500–900 RPM), feed rate (0.15–0.25 mm/rev), and depth of cut (0.5–1.5 mm)—which were analyzed across three responses: average tool wear rate (mg/mm), surface roughness (mm), and material removal rate (mm^3/min). The simplex lattice design reduced the experimental runs to 16 blends, efficiently capturing the interactions among the variables.

During the cutting operation, a cylindrical rod (5 mm diameter, 150 mm length) was machined using a cermet insert under varying conditions to measure tool wear, surface roughness, and material removal rate. The setup involved clamping the workpiece in a chuck and adjusting the insert in the tool holder. Measurements were obtained using a non-contact video measuring system, a weighing balance, and a Surfcorder SE3500 surface tester. Figures illustrating both step-cut and parallel-cut turning operations were referenced to show the machining configurations.

Scanning Electron Microscope

A scanning electron microscope (SEM) is a type of electron microscope that produces images of a sample by scanning the surface with a focused beam of electrons. The electrons interact with atoms in the sample, producing various signals that contain information about the sample's surface topography and composition. The electron beam is scanned in a raster scan pattern, and the beam's position is combined with the detected signal to produce an image. SEM can achieve a resolution better than 1 nanometer. Specimens can be observed in high vacuum in conventional SEM, or in low vacuum or wet conditions in variable pressure or environmental SEM, and at a wide range of cryogenic or elevated temperatures with specialized instruments. (Stokes, 2008, and Wikipedia). For this, the scanning electron microscopy (SEM) was performed to examine the physical structure change of samples using the SEM model Phenom ProX, by Phenom World Eindhoven, the Netherlands. The sample was placed on a double adhesive, which was on a sample stub, was coated sputter coater by Quorum Technologies model Q150R, with 5nm of gold. Thereafter, it was taken to the chamber of the SEM machine, where it was viewed via NaVCaM for focusing and a little adjustment. It was then transferred to SEM mode, focused, and brightness contrast was automatically adjusted; afterward, the morphologies of different magnifications were stored in a USB stick.

Energy Dispersive X-Ray Spectroscopy (EDX)

Energy Dispersive X-Ray Spectroscopy (EDX) is an analytical technique used for elemental analysis or chemical characterization of a sample. It relies on the investigation of an interaction of some source of X-ray excitation and a

sample. In this study, Energy Dispersive X-Ray Spectroscopy (EDX) is conducted on the optimal sample, and the result of the characterization is presented in the results section.

RESULT AND DISCUSSION

X-ray Diffraction Analysis (XRD)Test Results

An XRD pattern was obtained for the thermally treated and the untreated composites. The XRD was the major analytical tool in this work, used to determine the various phases formed at different heat treatment conditions. Figure 1 shows the XRD pattern of the unreinforced alloy. From Figure 1, it was observed that the major diffraction peaks of the unreinforced alloy lie between 38-47 and 65-84 and the phases at these peaks are: Aluminium (α-Al), Aluminium magnesium (Al3 Mg2), magnesium silicon (Mg2 S), magnesium aluminium (Mg2 Al3), Aluminium magnesium (Al12 Mg1), and Al Mg. This is expected because the major alloying elements in A356 alloy are: Al, Si, and Mg. It clearly shows that the phases with magnesium are more than those of silicon. This may be attributed to the lower melting point of Magnesium than silicon, which resulted in the melting of the Mg and formation of a bond with the Al. From Table 1, it can be seen that Aluminium (α-Al) has the highest score of all the phases.

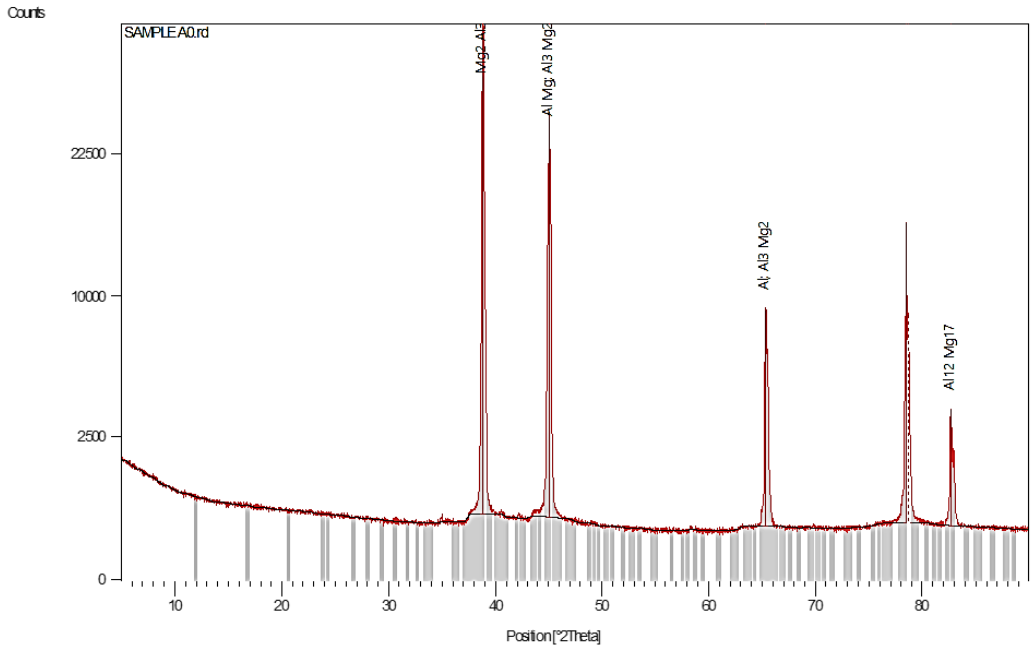

Figure 1. XRD Pattern of the A356 Alloy

Table 1. Identified Patterns List of the A356 Alloy

Visible	Ref. Code	Score	Compound Name	Displacement [°2Th.]	Scale Factor	Chemical Formula
*	01-1180	38	Aluminum	0.000	0.171	Al
*	11-	12	Aluminum	0.000	0.024	Al Mg

	0571		Magnesium			
*	18-0034	6	Aluminum Magnesium	0.000	0.208	$Al_3 Mg_2$
*	34-0458	3	Magnesium Silicon	0.000	0.007	$Mg_2 Si$
*	01-1132	5	Magnesium Aluminum	0.000	0.338	$Mg_2 Al_3$
*	73-1148	3	Aluminum Magnesium	0.000	0.031	$Al_{12} Mg_{17}$

Figure 2 displays the XRD patterns of the composites with CHp. The graph shows the presence of silicon oxide (SiO2), calcium carbonate (CaCO3), magnesium aluminum oxide (Mg Al2O4), sapphirine-2\ITM\RG (Mg3.5 Al9 Si1.5 O20) can be observed from the XRD pattern of the composites. The phases formed are as a result of CHp, which contains: silicon oxide (SiO2), calcium carbonate (CaCO3), silicon (Si) (see Table 2). It may be noted that these phases are in conformity with the works of Atuanya and Aigbodion (2014), using biomass, figures 1 and 2 refer. The possible interfacial reaction in the composites is given in the equation.

$$2SiO_2(s) + 2Al(l) + Mg(l) \leftrightarrow MgAl_2O_4(s) + 2Si(s) \ (\Delta G = -36.4 \text{ kJ/kg at } 1000 \text{ K}) \ldots \text{(Eqn. 1)}$$

Similar observations have been made by Rajan et al (2007) on commercially pure Al alloy reinforced with fly ash. It should be noted that the presence of CHp in the composite resulted in a much smaller grain size when compared with the matrix alloy. In these diffractograms, one can evidently differentiate the crystalline phases of the master alloy from those of the composite material.

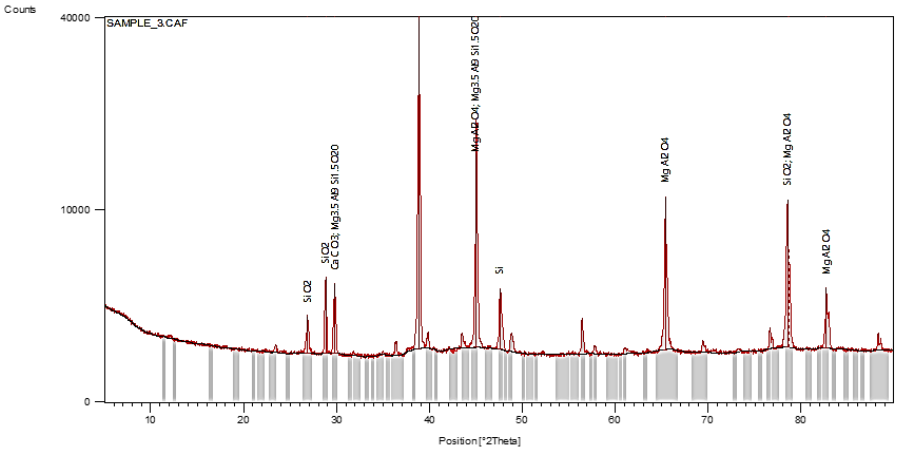

Figure 2. XRD Pattern of the A356 Alloy with 10wt%CHp (Adopted from Ochieze, 2017)

Table 2. Identified Patterns List of the Composites

Visible	Ref. Code	Score	Compound Name	Displacement [°2Th.]	Scale Factor	Chemical Formula
*	81-0068	38	Silicon Oxide	0.000	0.067	SiO_2
*	29-	34	Calcium	0.000	0.066	$CaCO_3$

	0305		Carbonate			
*	83-2468	33	Quartz, syn	0.000	0.024	SiO_2
*	10-0062	21	Magnesium Aluminum Oxide	0.000	0.241	$MgAl_2O_4$
*	80-0018	28	Silicon	0.000	0.038	Si
*	21-0549	14	Sapphirine-2\ITM\RG	0.000	0.050	$Mg_{3.5}$ Al_9 $Si_{1.5}$ O_{20}

Morphology Test Results - Scanning Electron Microscope (SEM)

The SEM observation validates that the adhesion of the debris is mainly accountable for the higher wear. It is noteworthy that the frictional force increased when the sliding velocity was increased at a constant load. Hence, higher interfacial temperature induced by frictional heat loosens the bonding at the interface between the Al alloy matrix and CHp reinforcement particles, resulting in higher plastic deformation. The improvement in the wear resistance of the composites may be attributed to the toughening effect due to the incorporation of larger cow horn particles in the matrix. The SEM observation supports the fact that the wear of the composites is lower than that of the alloy.

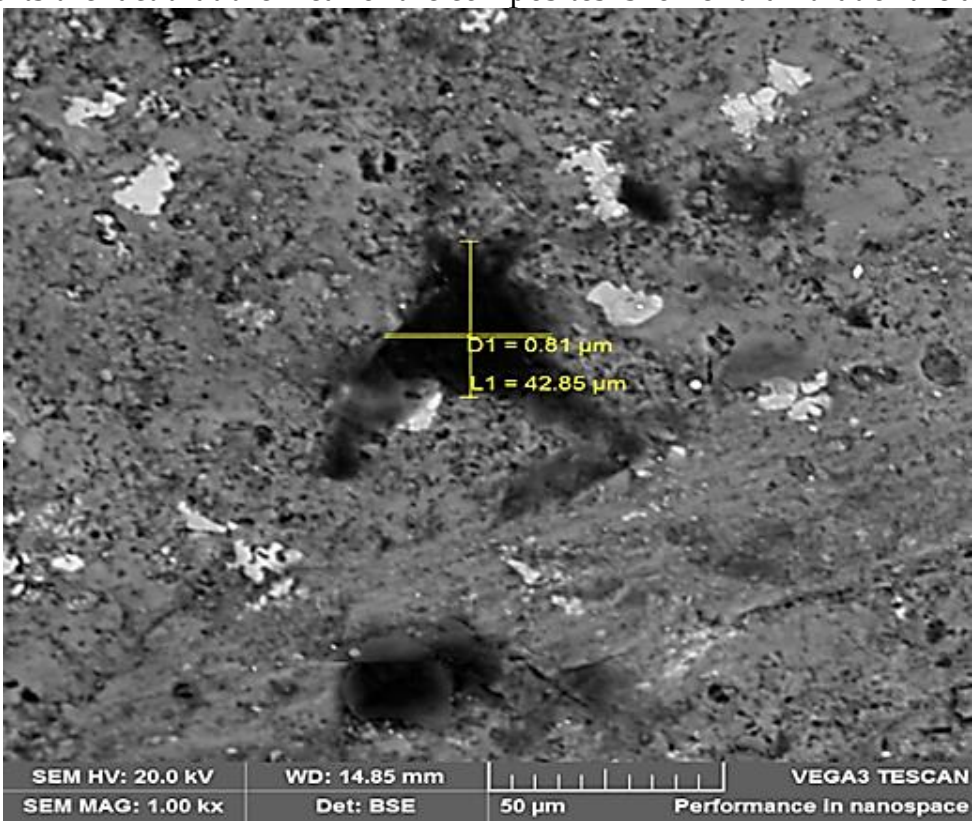

Figure 3. SEM of Worn Surface of A356 Alloy

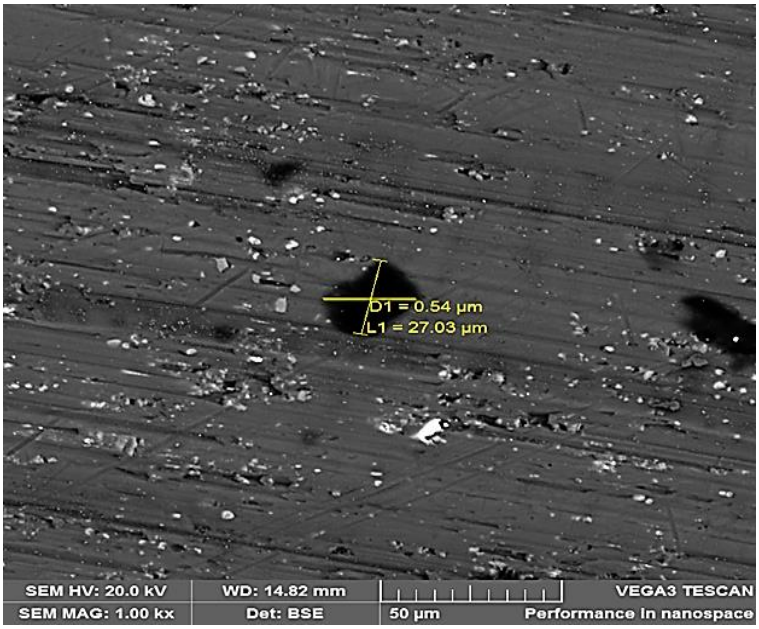

Figure 4. SEM of Worn Surface of A356 Alloy/10wt%CHp

The X-ray Diffraction (XRD) and Scanning Electron Microscope (SEM) analyses provided a comprehensive understanding of the phase composition and microstructural behavior of the A356 aluminum alloy and its cow horn particulate (CHp) reinforced composites. The XRD pattern of the unreinforced A356 alloy revealed prominent peaks between 38–47° and 65–84°, corresponding to phases such as α-Al, Al_3Mg_2, Mg_2Si, Mg_2Al_3, $Al_{12}Mg_{17}$, and AlMg. This result indicates the dominance of aluminum-magnesium intermetallics due to magnesium's lower melting point and its strong affinity for aluminum, a finding that agrees with Zhang et al. (2023), who reported similar Al-Mg phase formation in thermally treated aluminum-silicon alloys. In contrast, Pu et al. (2025) observed higher silicon phase formation when Mg concentration was reduced, suggesting the compositional balance of Mg and Si strongly influences intermetallic bonding.

For the CHp-reinforced composites, XRD patterns showed additional peaks of SiO_2, $CaCO_3$, $MgAl_2O_4$, and Sapphirine-2($Mg_{3.5}Al_9Si_{1.5}O_{20}$), confirming successful chemical interaction between the organic reinforcement and metallic matrix. These findings are in line with Kumar, M. S. (2023), who noted that the inclusion of bio-waste reinforcements such as bone ash or horn particulates introduces stable oxides that improve hardness and wear resistance. In a related study, Wang et al (2019) also found that $MgAl_2O_4$ spinel formation enhances interfacial bonding between the reinforcement and matrix, resulting in fine-grain structures. However, unlike the results of Rong et al. (2024), where excessive oxide formation led to brittleness in aluminum composites, the current study achieved an optimal oxide balance, maintaining toughness while refining grain boundaries.

The SEM analysis further validated these structural transformations. The unreinforced alloy displayed signs of plastic deformation and adhesive wear due to weak interfacial strength, while the CHp-reinforced composites showed smoother worn surfaces with fewer grooves, indicating reduced wear. This agrees with the report of Kumar et al. (2024), which demonstrated that organic

reinforcements in aluminum matrices act as barriers to dislocation and microcrack propagation. In contrast, Oladele et al. (2025) observed that smaller reinforcement particles tend to cluster, weakening the interface; however, the larger cow horn particulates used here improved bonding and wear resistance.

CONCLUSIONS AND RECOMMENDATIONS

The study on the microstructural and elemental characterization of Aluminium Alloy A356 reinforced with cow horn particulates (CHp) using Scanning Electron Microscopy (SEM) and Energy Dispersive X-ray Spectroscopy (EDX) techniques revealed significant structural and compositional improvements in the composite material. The SEM analysis confirmed a uniform distribution of CHp within the aluminum matrix, leading to refined grain structures, enhanced interfacial bonding, and reduced porosity. These features contributed to improved mechanical integrity and wear resistance when compared with the unreinforced A356 alloy. The EDX results further validated the successful incorporation of key elemental constituents such as carbon, calcium, silicon, magnesium, and oxygen, originating from the cow horn particles, which formed stable oxide and carbide phases. The interaction between aluminum and CHp resulted in the formation of intermetallic and oxide compounds such as $MgAl_2O_4$ and SiO_2, which strengthened the matrix and improved its thermal stability. The presence of these phases confirmed effective metallurgical bonding between the reinforcement and matrix, promoting load transfer efficiency during mechanical stress.

FURTHER RESEARCH

This research still has limitations, so further research on this topic is still needed.

REFERENCES

Atuanya, C. U., & Aigbodion, V. S. (2014). Evaluation of Al–Cu–Mg alloy/bean pod ash nanoparticles synthesis by double-layer feeding–stir casting method. Journal of alloys and compounds, 601, 251-259.

Kumar, A., Singh, V. P., Singh, R. C., Chaudhary, R., Kumar, D., & Mourad, A. H. I. (2024). A review of aluminum metal matrix composites: fabrication route, reinforcements, microstructural, mechanical, and corrosion properties. Journal of Materials Science, 59(7), 2644-2711.

Kumar, M. S. (2023). Utilizing bio-waste as the reinforcement particles for the production of sustainable composite brakes and the investigation of their tribological and corrosive performance. Environmental Science and Pollution Research, 30(3), 6935-6949.

Le, X. B., & Choa, S. H. (2024). Assessment of the Risk of Crack Formation at a Hybrid Bonding Interface Using Numerical Analysis. Micromachines, 15(11), 1332.

Nwobi-Okoye, C. C., & Ochieze, B. Q. (2018). Age hardening process modeling and optimization of aluminum alloy A356/Cow horn particulate composite for brake drum application using RSM, ANN, and simulated annealing. Defence Technology, 14(4), 336-345.

Nwobi-Okoye, C. C., Ochieze, B. Q., & Okiy, S. (2019). Multi-objective optimization and modeling of age hardening process using ANN, ANFIS, and genetic algorithm: Results from aluminum alloy A356/cow horn particulate composite. Journal of Materials Research and Technology, 8(3), 3054-3075.

Ochieze, B. Q., Nwobi-Okoye, C. C., & Atamuo, P. N. (2018). Experimental study of the effect of wear parameters on the wear behavior of A356 alloy/cow horn particulate composites. Defence technology, 14(1), 77-82.

Oguntuase, M., Adeyemi, G. J., & Stephen, J. T. (2022). Effects of Cow Horn Particulates as Addictive on Microstructure, Tensile, and Compressive Properties of Recycled Aluminium Alloy. European Journal of Engineering and Technology Research, 7(2), 146-152.

Oladele, I. O., Falana, S. O., Akinbamiyorin, M., Onuh, L. N., Taiwo, A. S., Adelani, S. O., & Olajesu, O. F. (2025). Cyclic thermal treatment parameters of bagasse particle reinforced epoxy bio-composites for sustainable applications. Discover Polymers, 2(1), 1-22.

Pu, C., Gao, X., Wu, Z., Du, Z., & Jing, Z. (2025). Metal-silicate partitioning of Si, O, and Mg at high pressures and high temperatures: Implications to the compositional evolution of core-forming metallic melts. Geochemistry, Geophysics, Geosystems, 26(2), e2024GC011940.

Rajan, T. P. D., Pillai, R. M., Pai, B. C., Satyanarayana, K. G., & Rohatgi, P. K. (2007). Fabrication and characterisation of Al–7Si–0.35 Mg/fly ash metal matrix composites processed by different stir casting routes. Composites Science and Technology, 67(15-16), 3369-3377.

Rong, X., Zhao, D., He, C., & Zhao, N. (2024). recent progress in aluminum matrix composites reinforced by in situ oxide ceramics. Journal of Materials Science, 59(22), 9657-9684.

Wang, F., Li, J., Shi, C., Liu, E., He, C., & Zhao, N. (2019). Orientation relationships and interface structure in MgAl2O4 and MgAlB4 Co-reinforced Al matrix composites. ACS Applied Materials & Interfaces, 11(45), 42790-42800.

Zhang, M., Tian, Y., Zheng, X., Zhang, Y., Chen, L., & Wang, J. (2023). Research progress on multi-component alloying and heat treatment of high strength and toughness Al–Si–Cu–Mg cast aluminum alloys. Materials, 16(3), 1065.